Protist, Vol. 157, 45—60, January 2006
http://www.elsevier.de/protis
Published online date 13 December 2005

Protist

ORIGINAL PAPER

Phylogeny of Marine Gregarines (Apicomplexa) — *Pterospora*, *Lithocystis* and *Lankesteria* — and the Origin(s) of Coelomic Parasitism

Brian S. Leander[a,1], Shane A.J. Lloyd[b], Wyth Marshall[b], and Stephen C. Landers[c]

[a]Canadian Institute for Advanced Research, Program in Evolutionary Biology, Departments of Botany and Zoology, University of British Columbia, Vancouver, BC, Canada V6T 1Z4,
[b]Departments of Botany and Zoology, University of British Columbia, Vancouver, BC, Canada V6T 1Z4
[c]Department of Biological and Environmental Sciences, Troy University, Troy, AL 36082, USA

Submitted July 7, 2005; Accepted October 23, 2005
Monitoring editor: Frank Seeber

Gregarines constitute a large group of apicomplexans with diverse modes of nutrition and locomotion that are associated with different host compartments (e.g. intestinal lumena and coelomic cavities). A broad molecular phylogenetic framework for gregarines is needed to infer the early evolutionary history of apicomplexans as a whole and the evolutionary relationships between the diverse ultrastructural and behavioral characteristics found in intestinal and coelomic gregarines. To this end, we sequenced the SSU rRNA gene from (1) *Lankesteria abbotti* from the intestines of two Pacific appendicularians, (2) *Pterospora schizosoma* from the coelom of a Pacific maldanid polychaete, (3) *Pterospora floridiensis* from the coelom of a Gulf Atlantic maldanid polychaete and (4) *Lithocystis* sp. from the coelom of a Pacific heart urchin. Molecular phylogenetic analyses including the new sequences demonstrated that several environmental and misattributed sequences are derived from gregarines. The analyses also demonstrated a clade of environmental sequences that was affiliated with gregarines, but as yet none of the constituent organisms have been described at the ultrastructural level (apicomplexan clade I). *Lankesteria* spp. (intestinal parasites of appendicularians) grouped closely with other marine intestinal eugregarines, particularly *Lecudina tuzetae*, from polychaetes. The sequences from all three coelomic gregarines branched within a larger clade of intestinal eugregarines and were similarly highly divergent. A close relationship between *Pterospora schizosoma* (Pacific) and *Pterospora floridiensis* (Gulf Atlantic) was strongly supported by the data. *Lithocystis* sp. was more closely related to a clade of marine intestinal gregarines consisting of *Lankesteria* spp. and *Lecudina* spp. than it was to the *Pterospora* clade. These data suggested that coelomic parasitism evolved more than once from different marine intestinal eugregarines, although a larger taxon sample is needed to further explore this inference.

Key words: Apicomplexa; gregarines; *Lankesteria*; *Lithocystis*; *Pterospora*; coelomic parasitism; evolution; phylogeny; SSU rDNA.

Introduction

Gregarine life cycles include distinctive extracellular trophozoite stages that inhabit the body

[1]Corresponding author;
fax +1 604 822 6089
e-mail bleander@interchange.ubc.ca (B.S. Leander)

doi:10.1016/j.protis.2005.10.002

cavities of invertebrates (e.g. annelids, molluscs, nemerteans, sipunculids, phoronids, crustaceans, echinoderms, hemichordates, appendicularians and insects). The trophozoites of most gregarines attach to epithelial tissues and occupy the gut lumena of their hosts. Many other gregarines, however, can be encountered in coelomic cavities and spaces associated with host reproductive systems (e.g. gonads, seminiferous vesicles and a variety of reproductive ducts). When two trophozoites are observed joined together just before sex, a process called syzygy, the two cells are referred to as gamonts. The orientation of gamonts during syzygy differs in different species; for instance, gamonts can be joined head-to-head, tail-to-tail, head-to-tail and side-to-side. A robust wall forms around the gamonts forming a gametocyst, within which several rounds of mitosis produce hundreds of gametes (gamotogony). Zygotes (the fleeting diploid stage) are formed after one gamete from each gamont fuse together. A sporocyst wall forms around each zygote, which rapidly undergoes meiosis producing 4 or more infective sporozoites within each sporocyst (note: 'oocyst' has been used synonymously with 'sporocyst' in gregarine literature). Gametocysts filled with sporocysts are released into the environment either by way of host feces (for intestinal gregarines), host gametes (for gonadal gregarines) or host disintegration (coelomic gregarines). New host organisms inadvertently consume sporocysts in their environment. After entering the intestinal tract, the infective sporozoites are released from sporocysts and begin to feed, grow and eventually develop into trophozoites within the intestinal lumen. The sporozoites of coelomic and gonadal gregarines make their way into the appropriate host body cavity before developing into trophozoites. In some gregarines (e.g. neogregarines and archigregarines), the trophozoites increase their population sizes within the host by dividing asexually (merogony).

Trophozoites are the largest and most conspicuous stage in gregarine life cycles and are remarkably diverse both ultrastructurally and behaviorally. Correlations between trophozoite characteristics and the environment occupied within the host have been reported previously. For instance, the trophozoites of many intestinal gregarines, particularly the 'eugregarines' (e.g. *Lecudina*, *Lankesteria* and *Gregarina*; Fig. 1), tend to be large inflexible cells with a distinct anterioposterior axis and numerous epicytic folds arranged longitudinally over the cell surface (Heller and Weise 1973; Leander et al. 2003b; Levine 1976, 1977b; Vavra and Small 1969). The edges of these folds are thought to facilitate gregarine gliding motility by providing skate-like surfaces for an actinomyosin based motor system to operate against the substrate (Heintzelman 2004; Morrissette and Sibley 2002). Gliding might also be accomplished when some folds take the form of sinusoidal waves, whereby oblique planes of the folds move from front to back pushing against a layer of mucus (Vavra and Small 1969; Vivier 1968). Other intestinal gregarines, particularly the 'archigregarines' (e.g. *Selenidium*), have more flexible trophozoites with fewer or no epicytic folds. These trophozoites are incapable of gliding and instead move by perpetual writhing and bending (Mellor and Stebbings 1980; Stebbings et al. 1974). Evidence suggests that the trophozoites of archigregarines and eugregarines have very different modes of feeding: myzocytosis via an apical complex in the former and surface nutrition (pinocytosis) via widely scattered micropores in the latter (Dyson et al. 1994; Schrével 1968; Vivier 1968; Vivier and Schrével 1964; Warner 1968). These different feeding modes help explain the fundamental differences in surface morphology and patterns of motility in archigregarines and eugregarines.

Like archigregarines, trophozoites that inhabit coeloms, particularly the urosporidians (e.g. *Urospora*, *Pterospora* and *Lithocystis*; Fig. 2), and body cavities associated with the host's reproductive system (e.g. *Monocystis*, *Nematocystis* and *Rhynchocystis*) lack gliding motility and instead move by peristalsis or pulsation (Brownell and McCauley 1971; Coulon and Jangoux 1987; Landers 1991, 2001; Landers and Gunderson 1986; Landers and Leander 2005; MacMillan 1973; Warner 1968). The trophozoites of some urosporidians (e.g. *Pterospora* and *Lithocystis*) lack attachment structures (e.g. a mucron or epimerite) and are adorned with irregular surface crenulations, pits and ridges rather than a regular arrangement of epicyctic folds (Coulon and Jangoux 1987; Landers and Leander 2005). The extreme morphological differences between some urosporidians and intestinal eugregarines have made the evolutionary history of urosporidians very difficult to infer.

A fundamental goal of this research is to place trophozoite diversity into a molecular phylogenetic context in order to better understand the earliest stages in apicomplexan evolution and the origin(s) of different parasitic lifestyles in gregarines. This phylogenetic context is just beginning to take

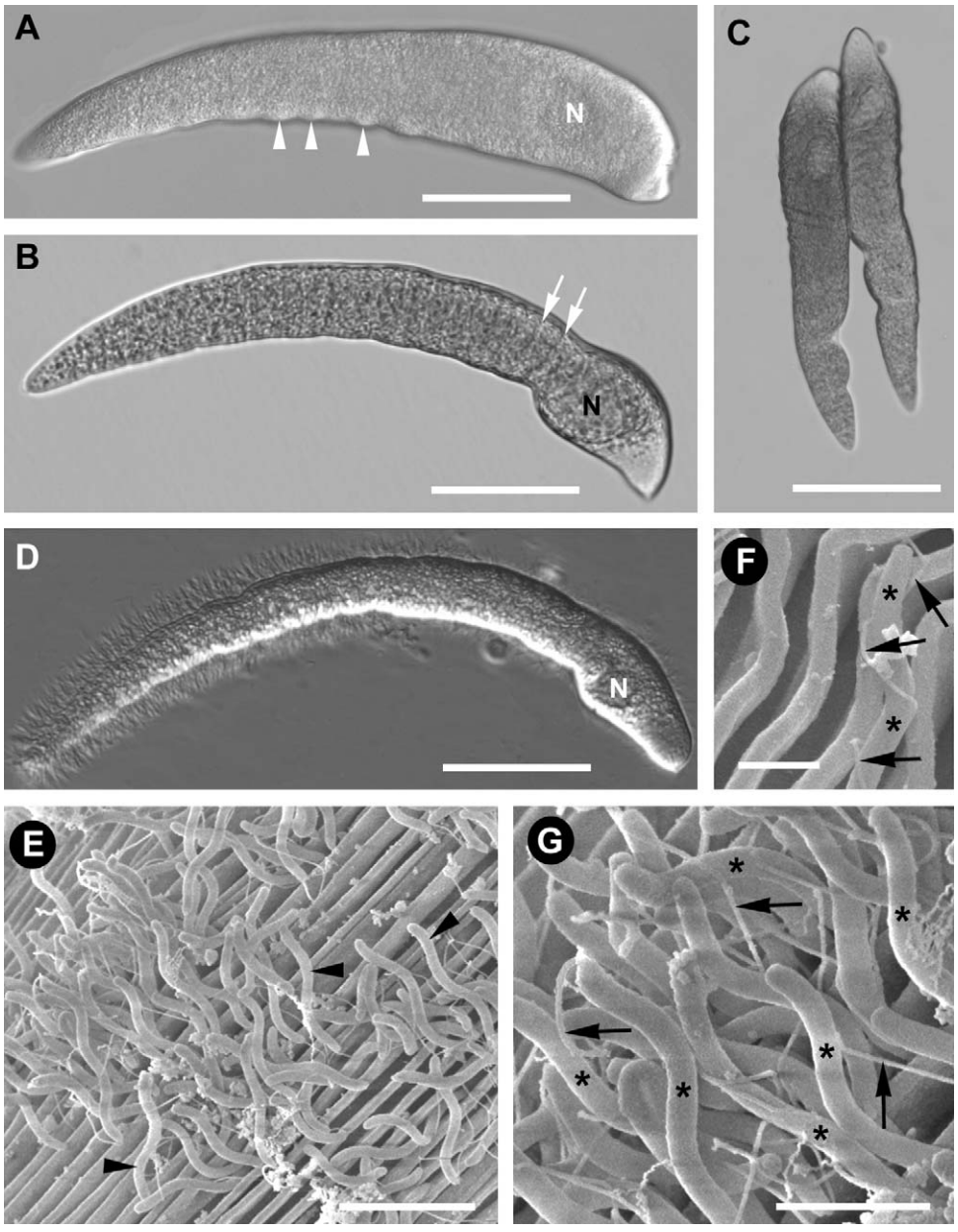

Figure 1. Trophozoites of *Lankesteria abbotti* isolated from the intestines of two appendicularians, *Cnemidocarpa finmarkiensis* and *Clavelina huntsmani*. **A.** Differential interference contrast (DIC) micrograph showing the anteriorly positioned nucleus (N) and a distinctive wrinkled concave margin (arrowheads). Bar = 30 μm. **B.** Phase contrast micrograph showing the anteriorly positioned nucleus (N) and two transverse ridges (arrows) on the cell surface. Bar = 30 μm. **C.** Phase contrast micrograph showing two trophozoites joined at the wrinkled concave margins of each cell (anterior ends up), an association reminiscent of gamonts in syzygy. Bar = 60 μm. **D.** Phase contrast micrograph showing motile filaments extending from the surface of a trophozoite (N, nucleus). Bar = 30 μm. **E.** Scanning electron micrograph (SEM) showing the motile filaments (arrowheads) extending from the longitudinal epicytic folds of a trophozoite. Bar = 2.5 μm. **F.** SEM showing that each motile filament consists of a thin flagellum (arrows) winding around a thick head element (asterisks). This morphology is consistent with that of appendicularian spermatozoa. Bar = 0.5 μm. **G.** SEM showing several appendicularian spermatozoa, each consisting of a thick head element (asterisks) and a thin flagellum (arrows). Bar = 1 μm.

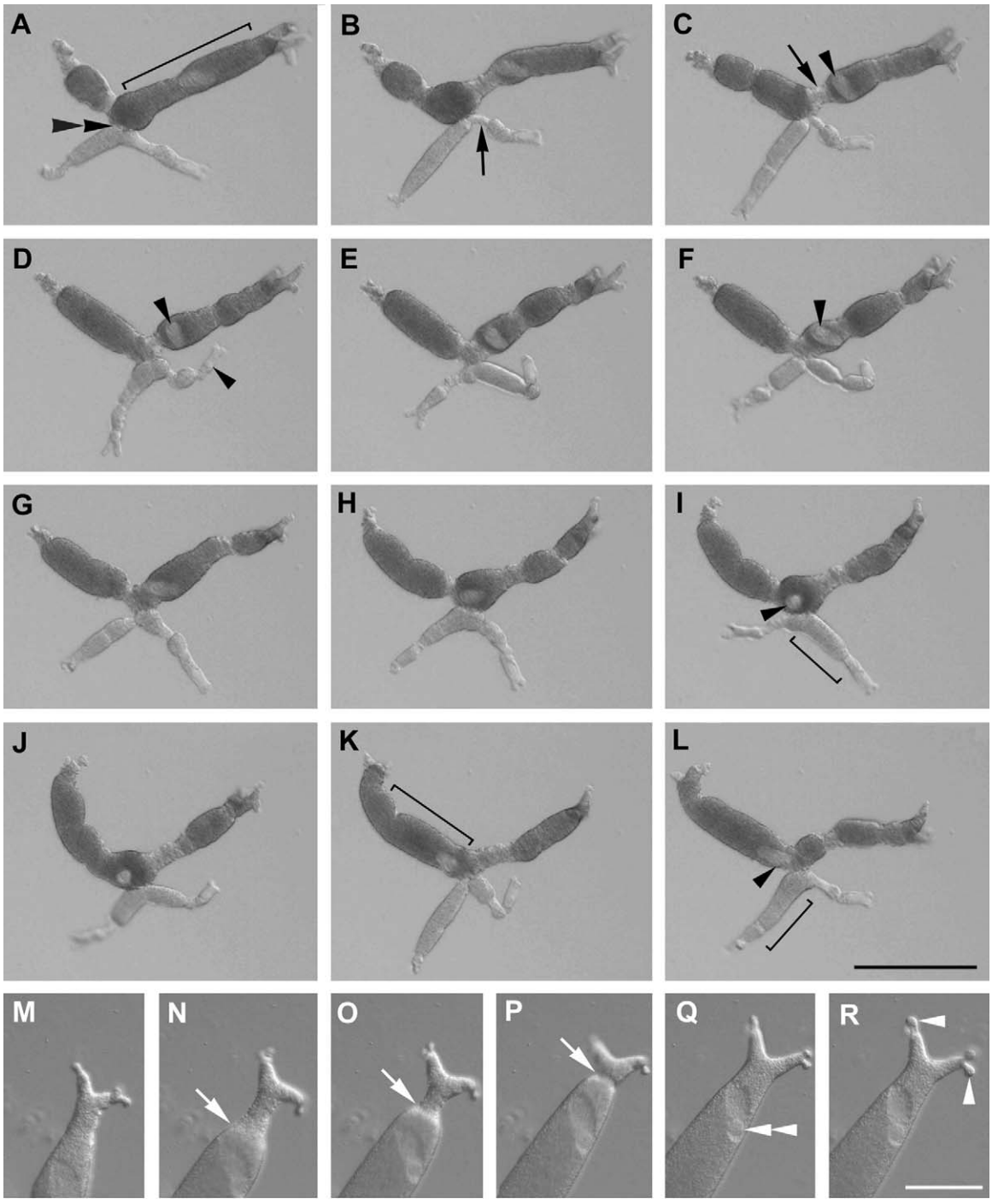

Figure 2. Gamonts of *Pterospora schizosoma* isolated from the coelomic spaces of a maldanid polychaete, *Axiothella rubrocincta*. **A—L.** A time series of differential interference contrast (DIC) micrographs (1 frame/s) showing the peristaltic movements of two gamonts in syzygy. Each gamont is V-shaped, consisting of a short soma and two long trunks (brackets) that bifurcate into smaller terminal digits. Gamonts join to one another at the base of each V-shaped cell (double arrowhead). Constricted regions in the cell (arrows) move toward the terminal digits and push cytoplasm and nuclei (arrowheads) along the length of each trunk. Bar = 50 μm. **M—R.** A time series of differential interference contrast (DIC) micrographs (1 frame/s) showing the cytoplasm and nucleus (with nucleolus — double arrowhead) being pushed towards and into the terminal digits (arrowheads) by a constricted cell region (arrow). Bar = 5 μm.

shape as small subunit (SSU) rDNA sequences from gregarines are being generated from environmental sequence surveys and manually isolated trophozoites and gametocysts extracted from marine invertebrate hosts (Carreno et al. 1999; Dawson and Pace 2002; Edgcomb et al. 2002; Leander et al. 2003a, b, c; Leander and Keeling 2004; Lopez-Garcia et al. 2001; Moreira and López-García 2002). Previous reports suggest that colpodellids (myzocytotic biflagellated predators with an apical complex, e.g. *Colpodella*) and archigregarines (e.g. *Selenidium*) diverge near the nexus of the early apicomplexan radiation and that eugregarines and neogregarines form a clade that is separate from all other apicomplexans (i.e. coccidians and piroplasmids) (Cavalier-Smith and Chao 2004; Kuvardina et al. 2002; Leander and Keeling 2003; Leander et al. 2003c). These molecular phylogenetic data along with analyses using several protein-coding genes also suggest that the important vertebrate intestinal parasite *Cryptosporidium* has a closer phylogentic affinity to gregarines than to other vertebrate apicomplexan parasites (Carreno et al. 1999; Leander et al. 2003a, b; Leander and Keeling 2004). This insight could have a profound impact on *Cryptosporidium* research and our understanding of the possible convergent evolution of vertebrate intestinal parasitism by apicomplexans. The addition of SSU rDNA sequences from known gregarines (and colpodellids) has also provided a basis for identifying sequences derived from environmental sequencing surveys and sequences that have been misattributed to other organisms (e.g. foraminiferans and metazoans) (Cavalier-Smith 2004; Leander et al. 2003a, c; Moreira and Lopez-Garcia 2003).

We were interested in expanding these data by exploring the molecular phylogeny of intestinal gregarines of appendicularians, namely *Lankesteria abbotti* (Pacific coast), and the following coelomic gregarines (Urosporida): *Pterospora schizosoma* from the maldanid polychaete *Axiothella rubrocincta* (Pacific coast), *Pterospora floridiensis* from the maldanid polychaete *Axiothella mucosa* (Gulf of Mexico) and *Lithocystis* sp. from the echinoid echinoderm *Brisaster latifrons* (Pacific coast). We addressed (1) the relationship of *Lankesteria* species to different *Lecudina* species, (2) whether coelomic gregarines form a monophyletic group or have exploited coelomic environments several times independently and (3) the phylogenetic position of coelomic gregarines relative to archigregarines, eugregarines and neogregarines. The new sequences enabled us to positively identify several environmental sequences and misattributed sequences in GenBank as close relatives of known gregarines. The emerging molecular phylogenetic framework allowed us to infer patterns of character evolution within gregarines and to highlight important areas of uncertainty that should help guide future research on gregarine diversity.

Results

Morphological Characteristics of *Lankesteria abbotti*

The trophozoites of *L. abbotti* were found attached to the epithelial lining of appendicularian intestines and had a characteristic crescent shape with a wrinkled concave margin (Fig. 1A—D). The length of the trophozoites ranged from 130—160 μm ($n = 20$). The anterior end of the cell contained the nucleus and was usually demarcated by a swollen head-like region that terminated with a relatively pointed mucron (Fig. 1B and D). Transverse ridges (syn. pseudosepta) were occasionally observed near the base of the head-like anterior end (Fig. 1B). The posterior end of the cell tapered to a blunt point. Syzygy was observed side-to-side, and gamonts were joined at their anterior concave margins (near the position of the nuclei); the posterior regions of the wrinkled margins were oriented medially (Fig. 1C). Trophozoites were capable of gliding motility and the cell surface was adorned with numerous longitudinal epicytic folds (Fig. 1E and F). Some trophozoites were covered with highly motile filaments (Fig. 1D). Scanning electron microscopy demonstrated that these filaments were not produced by the trophozoites, but instead were the sperm of the appendicularian host attached to the trophozoite surface (Fig. 1E—G). The sperm consisted of a thick head region and a long thin flagellum.

Morphological Characteristics of Urosporidians

The light microscopical and ultrastructural features of trophozoites from *P. schizosoma* and *P. floridiensis* have been reported previously (Landers 2001; Landers and Gunderson 1986; Landers and Leander 2005). Figure 2 highlights the general appearance and pulsating movements of *P. schizosoma* gamonts in syzygy. Writhing gamont pairs were found in the coelomic fluid of

maldanid polychaetes and were unattached to the host peritoneal lining. About one in six hosts were infected with *P. schizosoma* ($n = 62$). When infected, only a few gamont pairs (1—7) were found in any one host, but the coelomic spaces were usually heavily populated with gametocysts. The number of gametocysts per individual host varied considerably (e.g. 10 to over 100) and presumably was correlated with the relative age of the host, where older worms had more gametocysts stored within their coloemic spaces. Each gamont had the characteristic V-shaped (*P. schizosoma*) or Y-shaped (*P. floridiensis*) cell morphology, and accordingly, gamont pairs were X-shaped (Fig. 2A—L). The trunks of each gamont bifurcated repeatedly into terminal digits, where the number of terminal digits differs in different species. Peristaltic-like waves of constricted cell regions pushed cytoplasm and the large nucleus throughout the cell; the cytoplasm was usually forced from one trunk to the other in an alternating pattern (Fig. 2A—L). The terminal digits were sequentially inflated and deflated as the cytoplasm was pushed into and out of each trunk (Fig. 2M—R).

The trophozoites of *Lithocystis* sp. were not observed. Our designation is consistent with Brownell and McCauley (1971), who reported that the commonest gregarines inhabiting the perivisceral coelom of *B. latrifrons* were several species of *Lithocystis*.

Molecular Phylogeny of Gregarines as Inferred from SSU rDNA

The phylogenetic topology shown in Figure 3 recovered three major clades: (1) ciliates, (2) dinoflagellates plus *Perkinsus* and (3) apicomplexans plus *Colpodella*. Although the third clade was weakly supported by the data, it is consistent with analyses reported previously (Cavalier-Smith and Chao 2004; Kuvardina et al. 2002; Leander et al. 2003b, c). The sequence from the archigregarine *Selenidium terebellae* clustered with an environmental sequence (AF372780) and both formed a sister group to all of the other sequences within the apicomplexan clade, albeit with weak statistical support. A clade of *Cryptosporidium* sequences formed the sister group to a weakly supported clade containing all of the other gregarine sequences in the analysis, namely the neogregarines and eugregarines, and a clade of sequences from organisms that have yet to be described at the ultrastructural level: 'undescribed apicomplexan clade I' (Fig. 3). The eugregarine *Monocystis agilis* from the seminiferous vesicles of earthworms (*Lumbricus terrestris*) and a closely related environmental sequence (AY179988) clustered with a clade of neogregarines isolated from insect hosts. This relationship was bolstered by a signature nucleotide at position 453 (relative to the SSU rDNA sequence from *S. terebellae*). The remaining eugregarine sequences formed a moderately supported clade containing septate gregarines from the intestinal tracts of insects (*Gregarina* and *Leidyana*), aseptate gregarines from the intestinal tracts of marine polycheates (*Lecudina*), aseptate gregarines from the intestinal tracts of appendicularians (*Lankesteria*) and aseptate gregarines isolated from the coelomic spaces of marine polychaetes and echinoderms (*Pterospora* and *Lithocystis*) (Fig. 3). This clade of intestinal and coelomic eugregarines was bolstered by signature nucleotides at positions 1369 and 1603 (relative to the SSU rDNA sequence from *S. terebellae*). The sequences from vertebrate parasites, namely coccidians (except *Cryptosporidium*) and piroplasmids, formed a moderately supported sister clade to the group of sequences containing cryptosporidians, eugregarines, neogregarines and apicomplexan clade I.

The coelomic gregarines *P. schizosoma* (Pacific coast) and *P. floridiensis* (Gulf of Mexico) formed a strongly support clade that was deeply nested within sequences from intestinal gregarines possessing numerous epicytic folds and gliding motility (e.g. *Gregarina*, *Leidyana*, *Lecudina* and *Lankesteria*) (Fig. 3). The coelomic gregarine *Lithocystis* sp. (Pacific coast) diverged after the *Pterospora* clade and formed a sister lineage to a clade containing sequences from *Lecudina* and *Lankesteria*. An environmental sequence (AY179977) clustered strongly with the sequence from *Lecudina tuzetae*. A sequence attributed to the appendicularian *Clavelina picta* (Atlantic coast) in GenBank (AY116614) clustered strongly with *L. abbotti*, which was isolated from two Pacific appendicularians, *Cnemidocarpa finmarkiensis* and *Clavelina huntsmani*. The clade containing coelomic gregarines (*Pterospora* and *Lithocystis*) and the marine intestinal gregarines *Lankesteria* spp. and *L. tuzetae* was strongly supported by the data (Fig. 3). The closest sister lineage to this clade was *Lecudina polymorpha*, which was isolated from the intestines of the marine polychaete *Lumbrineris*. The clade of marine eugregarines (ancestor '**M**' and all of its descendants in Fig. 3; *Lecudina*, *Lankesteria*, *Pterospora* and *Lithocystis*) was bolstered by signature

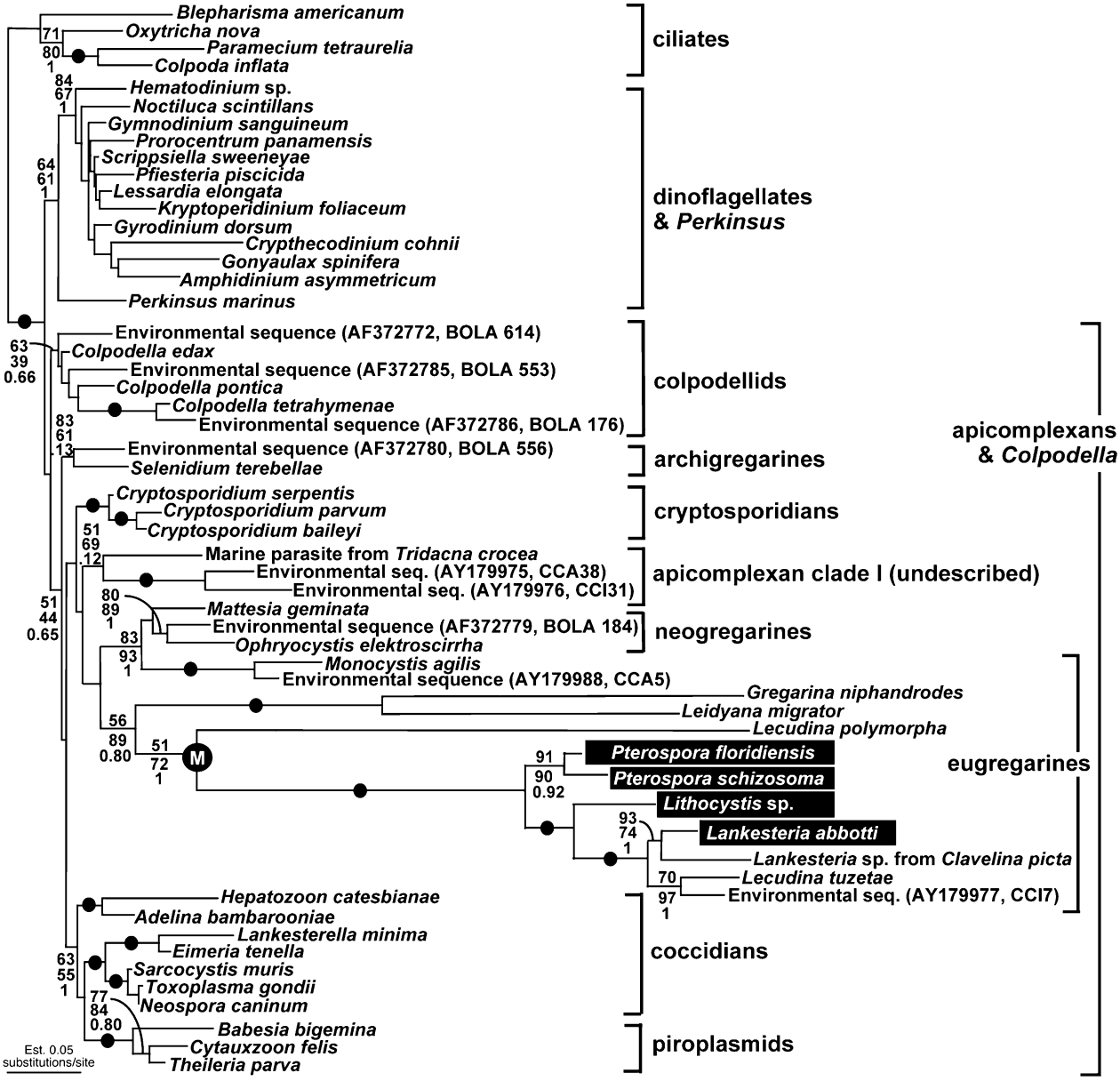

Figure 3. Gamma-corrected maximum likelihood tree ($-\ln L = 15{,}113.492$, $\alpha = 0.37$, number of rate categories = 8) inferred using the GTR model of substitution on an alignment of 56 SSU rDNA sequences and 1163 sites. Numbers at the branches denote gamma-corrected bootstrap percentages using maximum likelihood — HKY (upper) and weighted neighbor-joining (middle). The lower number refers to Bayesian posterior probabilities — GTR. Black dots on branches denote bootstrap values and posterior probabilities above 90% in all analyses. SSU rDNA sequences generated from this study are highlighted in black boxes. The letter "**M**" refers to the most recent common ancestor of all *marine* eugregarines (*Lecudina*, *Lankesteria*, *Pterospora* and *Lithocystis*). Organisms representing apicomplexan clade I have yet to be characterized at the ultrasructural level.

nucleotides at positions 98, 770, 806, 1054, 1739 and 1747 (relative to the SSU rDNA sequence from *S. terebellae*). As evident in Fig. 3, long branches were observed in all members of the clade containing intestinal and coelomic eugregarines (*Gregarina*, *Leidyana*, *Lecudina*, *Pterospora*, *Lithocystis* and *Lankesteria*). Therefore, artifacts caused by long branch attraction (LBA)

cannot be ruled out for the deep nodes relating septate gregarines (*Gregarina* and *Leidyana*), *L. polymorpha* and the clade containing *Pterospora*, *Lithocystis* and *Lankesteria*.

Discussion

Character Evolution in Gregarines

Trophozoites are the most conspicuous and morphologically diverse stage in gregarine life cycles. The trophozoites of marine archigregarines are considered to have retained several ancestral characteristics that provide important insights into the earliest stages in apicomplexan evolution (e.g. intestinal parasitism, myzocytosis and an apical complex with a closed conoid)(Grassé 1953; Leander et al. 2003b; Leander and Keeling 2003; Levine 1971; Schrével 1971a, b). The trophozoite surfaces of most archigregarines (e.g. *Selenidium* and *Digyalum*) tend to have transverse striations and relatively few (0—50) longitudinally arranged epicytic folds (Dyson et al. 1993, 1994; Leander et al. 2003b; Levine 1971; MacGregor and Thomas 1965; Ray 1930; Schrével 1970, 1971a; Vivier and Schrével 1964, 1966). By contrast, the trophozoite surfaces of eugregarines have become highly folded in different ways in order to achieve new modes of feeding and cell locomotion within different host compartments (e.g. intestines and coelomic cavities). Although preliminary, the emerging molecular phylogenetic framework goes a long way in putting trophozoite diversity into an evolutionary context.

The following narrative can be inferred from the topology shown in Fig. 4. Myzocytosis-based feeding using an apical complex with an open 'conoid' (pseudoconoid) was the mode of nutrition present in the most recent common ancestor of dinoflagellates and apicomplexans (i.e. the Myzozoa)(Cavalier-Smith and Chao 2004; Kuvardina et al. 2002; Leander and Keeling 2003, 2004; Siddall et al. 2001). This combination of characters is found in modern colpodellids and perkinsids (Brugerolle 2002a, b; Brugerolle and Mignot 1979; Leander et al. 2003c; Mylnikov 1991, 2000; Mylnikov et al. 1998; Perkins 1976, 1996; Simpson and Patterson 1996). Colpodellids, archigregarines and cryptosporidians possess a four-way divisional cyst (e.g. four sporozoites per 'sporocyst' in the case of archigregarines and cryptosporidians) that ultimately gives rise to the feeding stages in the life cycle (Fig. 4, position 2). More derived gregarines (eugregarines and neogregarines) possess more than four sporozoites per sporocyst. The earliest diverging apicomplexans were archigregarines that exploited the intestinal lumena of marine invertebrates and, like colpodellids, have retained myzocytosis as their principal mode of feeding (Leander and Keeling 2003; Schrével 1968, 1970, 1971a, b). The ancestral open conoid became completely closed and flagella were secondarily lost in the infective sporozoite and trophozoite stages of apicomplexan life cycles (Fig. 4, position 3). Sexual reproduction in the earliest apicomplexans involved syzygy as seen in modern gregarines (Fig. 4, position 3).

We infer that an archigregarine stem group gave rise to cryptosporidians, which exploited a deep position relative to the intestinal microvilli of vertebrate hosts and developed two schizogonies to increase the population size of sporozoites within their hosts (Fig. 4, position 4). We posit that the archigregarine stem group also gave rise to the lineage uniting (eu)coccidians with piroplasmids (Fig. 4, position 15). Cryptosporidians and the (eu)coccidian/piroplasmid clade might represent two independent lineages that evolved in vertebrate hosts from different archigregarine ancestors. As indicated above, this 'archigregarine stem group hypothesis' makes sense from an organismal perspective, because archigregarines share several presumably plesiomorphic features with free-living colpodellids, such as myzocytosis four sporozoites per sporocyst, extracellular trophozoites with a relatively unfolded cortex and prevalence in marine environments (Leander and Keeling 2004). Our molecular phylogenetic results are also consistent with this hypothesis in that archigregarines (e.g. *S. terebellae*) are the earliest diverging lineages within the cryptosporidian/gregarine clade (albeit with weak support, Fig. 3). Alternatively, the stem group giving rise to gregarines, cryptosporidians and the (eu)coccidian/piroplasmid clade might be part of a larger paraphyletic group of coccidians (Cavalier-Smith and Chao 2004). Increased molecular sampling from archigregarines will shed considerable light onto these differing hypotheses for apicomplexan origins. Nonetheless, symbioses between vertebrates and the (eu)coccidian/piroplasmid clade led to different degrees of intracellular parasitism and in some cases, the secondary loss of the conoid (e.g. piroplasmids).

Eugregarines were almost certainly derived from an archigregarine stem group (Cox 1994; Grassé 1953; Leander et al. 2003b; Schrével 1971a, b). The earliest eugregarines were parasites of marine invertebrates and developed gliding motility and a

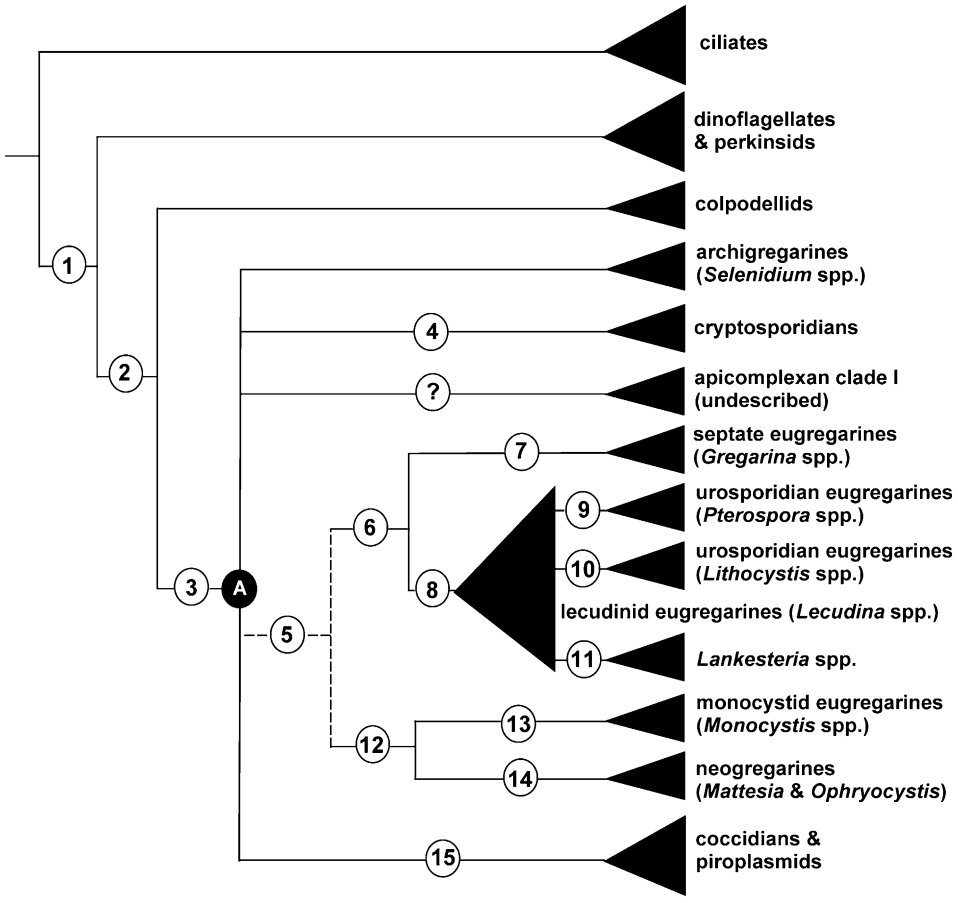

Figure 4. A synthetic phylogenetic framework based on current molecular sequence data, especially small subunit rDNA. Numbers indicate the inferred positions of character states as constrained by parsimony. The letter "A" refers to the most recent common ancestor of all apicomplexans. The "?" highlights our ignorance about the cellular identity of apicomplexan clade I. The dashed lines indicate the relative uncertainty regarding a hypothetical clade consisting of eugregarines and neogregarines. Although this putative clade is supported by morphological features (see below) and is frequently generated when all of the molecular data are used in phylogenetic analyses, the clade is not strongly supported by bootstrap statistics. The positions of some morphological and molecular characters inferred from this framework are as follows: **1** — apical complex with an open 'conoid' (pseudoconoid), myzocytosis-based feeding; **2** — four-way divisional cyst; **3** — apical complex with a closed conoid, syzygy and gamete formation, intestinal parasitism, trophozoites without flagella; **4** — intestinal parasites of vertebrates, two schizogonies, deep position relative to host microvilli; **5** — numerous (>50) longitudinally arranged epicytic folds, gliding motility via epicytic folds, loss of conoid in trophozoites, loss of myzocytosis; **6** — signature nucleotides at positions 1369 and 1603 relative to the SSU rDNA sequence from *Selenidium terebellae*; **7** — epicytic transverse septa between cell regions of trophozoites (e.g. protomerite and deutomerite), intestinal parasites of arthropods; **8** — signature nucleotides at positions 98, 770, 806, 1054, 1739 and 1747 relative to the SSU rDNA sequence from *Selenidium terebellae*; **9** — coelomic parasitism, trophozoite with pulsating/peristaltic cell motility, loss of epicytic folds and gliding motility in trophozoites, bifurcating cell shape with terminal digits, surface crenulations; **10** — coelomic parasitism, pulsating/peristaltic cell motility, loss of epicytic folds and gliding motility; **11** — intestinal parasites of chordates; **12** — signature nucleotide at position 453 relative to the SSU rDNA sequence from *Selenidium terebellae*; **13** — parasitism of reproductive vesicles and tubules in annelids, loss of gliding motility; **14** — non-intestinal parasites of insects; **15** — mainly intracellular parasites of vertebrates.

dense packing of longitudinally arranged epicytic folds (>50) that dramatically increased the surface area for the absorption of nutrients within intestinal environments (Heller and Weise 1973; Leander et al. 2003b; Vavra and Small 1969; Vivier 1968). The development of this mode of feeding co-occurred with the secondary loss of myzocytosis and the conoid in trophozoites (Fig. 4, position 5). The number of haploid sporozoites per sporocyst in eugregarines increased from 4 to 8 or more depending on the number of rounds of mitosis following meiosis (Levine 1976, 1977b). Although current taxon sampling is limited, our data suggests that a lecudinid stem group gave rise to all other eugregarine lineages and neogregarines (Fig. 4, position 5). A clade of marine eugregarines known as *Lankesteria* became specialized inhabitants of urochordates (Fig. 4, position 11). The intestinal eugregarines of insects became compartmentalized by forming epicytic transverse septa between cell regions and elaborate attachment structures (e.g. epimerites, protomerites and deutomerites) (Fig. 4, position 7). Some aseptate eugregarines, namely monocystids, became parasites of reproductive vesicles and tubules in annelids. The epicytic folds of these eugregarines became reduced or highly modified (e.g. *Nematocystis* and *Rhynchocystis*) and the loss of gliding motility was replaced by pulsating or peristaltic-like cell motility (MacMillan 1973; Warner 1968) (Fig. 4, position 13). Neogregarines, which are largely non-intestinal parasites of insects, appear to be closely related to monocystid eugregarines (Fig. 4, position 12).

Our data suggest that the occupation of host coelomic cavities by eugregarines might have occurred several times independently within a lecudinid stem group (Fig. 4, positions 9 and 10). Coelomic parasitism resulted following the traversal of sporozoites across the boundary formed by the closely associated intestinal wall and visceral peritoneal lining. The earliest coelomic eugregarines were probably similar to intestinal eugregregarines in morphology and behavior (e.g. *Urospora*). The trophozoites of more derived coelomic eugregarines (e.g. *Pterospora*) replaced epicytic folds and gliding motility for surface crenulations, peristaltic-like cell motility and a bifurcating cell shape with terminal digits (i.e. the gamonts are V-shaped or Y-shaped) (Landers 1991, 2001; Landers and Gunderson 1986; Landers and Leander 2005).

Modern coelomic eugregarines show intermediate character states associated with the morphological transformation from the highly folded, gliding trophozoites to crenulated, pulsating trophozoites. For instance, some coelomic eugregarines are attached to the inner peritoneal lining, creep (glide) along the coelomic wall and have a relatively dense packing of sinuous epicytic folds (e.g. *Urospora* spp.) (Coulon and Jangoux 1987). The vermiform trophozoites of *Lithocystis schneideri* have retained widely spaced epicytic folds but have abandoned gliding motility for pulsating motility within the coelomic fluid (Coulon and Jangoux 1987). Like *Pterospora* spp., the pear-shaped trophozoites of *Lithocystis foliacea* lacks epicytic folds altogether and exhibits pulsating cell motility. This species is covered with star-shaped ridges that are regularly spaced over the trophozoite surface (Coulon and Jangoux 1987). Different patterns of surface ridges and crenulations have also been found in different species of *Pterospora* (Landers and Leander 2005). Moreover, comparative data suggests that the X-shaped pattern of syzygy found in *Pterospora* spp. might be derived from the X-shaped side-to-side syzygies found in *Lithocystis* spp. (Coulon and Jangoux 1987). If so, the terminal ends of the V-shaped and Y-shaped gamonts in *Pterospora* (Fig. 1) would be best interpreted as modifications of the anterior and posterior ends of their mucron-bearing intestinal ancestors. This stands in contrast to the traditional interpretation that syzygy is head-to-head in *Pterospora*, as suggested by the elongated soma of *P. clymenellae* and *P. demodendrion* (Landers 1991; Levine 1977a). Overall, the highly unique characteristics of *Pterospora* spp. and *Lithocystis* spp. are inferred to be adaptations to the specific conditions present within the coeloms of metazoan hosts. Whether the similarities between certain species of *Pterospora* and *Lithocystis* are homologous or the result of evolutionary convergence remains to be tested with molecular phylogenies including in increased taxon sample.

Gregarines and Environmental Sequencing Surveys

Phylogenetic studies of randomly sequenced SSU rDNA from uncultured marine organisms have given rise to a broad array of unidentified lineages. These unidentified phylotypes are often thought to represent ‘novel’ organisms that are unknown to science (Dawson and Pace 2002; Diez et al. 2001; Edgcomb et al. 2002; Lopez-Garcia et al. 2001). However, several subsequent studies have elucidated the cellular identity of ‘novel’ lineages by

better characterizing known eukaryotes at both the molecular and cellular levels; this essentially increases the number of available reference taxa (Cavalier-Smith 2004; Leander et al. 2003a, c). Our results have added several additional reference points for interpreting environmental sequences. For instance, the following environmental sequences in GenBank can now be confidently attributed to specific gregarine clades: AF372779, AF372780, AY179975 and AY179988 (Berney et al. 2004) (Fig. 3). Apicomplexan clade I (AY179976, AY179977 and the *Tridacna* parasite) also appears to be closely related to gregarines, although the cellular identity of the group remains unclear (Fig. 3). Moreover, the phylogenetic position of our sequence from *L. abbotti* has demonstrated that the sequence attributed to *Clavelina picta* in GenBank (AY116614)(Stach and Turbeville 2002) is actually derived from a *Lankesteria* species parasitizing this appendicularian host.

Environmental sequencing surveys combined with studies like the one presented here have demonstrated that gregarine sporocysts are ubiquitous in marine sediments at all depths of the oceans (Berney et al. 2004; Cavalier-Smith 2004; Dawson and Pace 2002; Leander et al. 2003a; Moreira and Lopez-Garcia 2003; Wray et al. 1995). Nonetheless, the enormous void of molecular and ultrastructural data from gregarines continues to stifle any attempt to understand the diversity, prevalence, host specificity and geographic distribution of these parasites in marine environments. It is becoming increasingly obvious that interpreting the results of marine environmental sequence surveys will become appreciably more informative as knowledge of gregarines improves.

Methods

Collection of organisms: Host invertebrates were collected at low tide (0.2—0.3 m above the mean low tide) from several different locations in North America. Trophozoites from *Lankesteria abbotti* were isolated from the intestines of two appendicularians, *Cnemidocarpa finmarkiensis* and *Clavelina huntsmani*, collected in June 2004 from the rocky shores of Grappler Inlet near Bamfield Marine Sciences Centre, Vancouver Island (BC, Canada). These trophozoites conformed to the species description given by Levine (1981). Gametocysts and trophozoites from *Pterospora schizosoma* were isolated from the coelom of the bamboo worm, *Axiothella rubrocincta* (Polychaeta, Maldanidae), collected in August 2004 from Argyle Lagoon on San Juan Island (WA, USA). Gametocysts and trophozoites from *Pterospora floridiensis* were isolated from the coelom of the bamboo worm, *Axiothella mucosa* (Polychaeta, Maldanidae), collected in March 2004 from St. Andrew Bay (FL, USA). Gametocysts of *Lithocystis* sp. were isolated from the perivisceral coelom of the heart urchin, *Brisaster latifrons* (Echinodermata, Echinoidea, Spatangoidea) (Brownell and McCauley 1971), collected in July 2003 from dredged sediments in Barkley Sound near Bamfield Marine Sciences Centre, Vancouver Island (BC, Canada).

Light and electron microscopy: Host dissections and micromanipulation of individual trophozoites and gametocysts were conducted with a Leica MZ6 stereomicroscope, a Leica DMIL inverted microscope and a Zeiss Axiovert 200 inverted microscope. Differential interference contrast (DIC), Interference modulation contrast (IMC) and phase contrast light micrographs were produced by securing trophozoites under a cover slip with 'VALAP' [1 vaseline: 1 lanolin: 1 paraffin] and viewing them with either a Zeiss Axioplan 2 imaging microscope connected to a Leica DC500 color digital camera or the laboratories portable microscopy system consisting of a Leica DMIL inverted microscope connected to a PixeLink Megapixel color digital camera.

Trophozoites of *Lankesteria abbotti* were released into seawater by teasing apart the intestines of *Clavelina huntsmani* with fine-tipped forceps. Approximately 20 individual trophozoites were removed from the remaining gut material by micromanipulation and washed twice in filtered seawater. As described previously (Leander et al. 2003b), individual trophozoites were deposited directly into the threaded hole of a Swinnex filter holder, containing a 10 μm polycarbonate membrane filter (Coring Separations Division, Acton, MA) submerged in seawater within a small canister. Whatman filter paper, mounted on the inside base of a beaker, was used to fix the parasites with OsO_4 vapors for 30 min. Five drops of 4% OsO_4 (v/v) were added directly to the seawater and the trophozooites were fixed for an additional 30 min. The trophozoites were dehydrated with a graded series of ethyl alcohol and critical point dried with CO_2. Filters were mounted on stubs, sputter coated with gold, and viewed under a Hitachi S4700 Scanning Electron Microscope.

DNA extraction, PCR amplification, alignment and phylogenetic analysis: Fifty trophozoites of *Lankesteria abbotti* and over one hundred

gametocysts of both *Pterospora floridiensis* and *Pterospora schizosoma* were deposited into 1.5 ml Eppendorf tubes. Gametocysts of *Lithocystis* sp. were removed from the coelom of heart urchins using a hypodermic needle (20 gauge) and collected in a 1.5 ml Eppendorf tube. DNA was extracted with a standard CTAB extraction protocol: pelleted material was suspended in 400 μl CTAB extraction buffer (1.12 g Tris, 8.18 g NaCl, 0.74 g EDTA, 2 g CTAB, 2 g Polyvinylpyrolidone, 0.2 ml 2-mercaptoethanol in 100 ml water), homogenized in a Knotes Duall 20 tissue grinder, incubated at 65 °C for 30 min, and separated with chloroform:isoamyl alcohol (24:1). The aqueous phase was then precipitated in 70% ethanol.

Small subunit (SSU) rRNA genes from *Pterospora floridiensis*, *Pterospora schizosoma* and *Lankesteria abbotti* were amplified using PCR primers and a thermocycling protocol described previously for individually isolated gregarines (Leander et al. 2003a). 'Non-metazoan' PCR primers described by Bower et al. (2004) were used to amplify the SSU rDNA sequence from the inferred *Lithocystis* sp. PCR products corresponding to the expected size were gel isolated and cloned into the pCR 2.1 vector using the TOPO TA cloning kit (Invitrogen, Frederick, MD, USA). At least sixteen clones from each product were screened for size using PCR and digested with *Sau*3AI in order to group the products by restriction pattern. Two to four clones from each restriction pattern were sequenced with ABI bigdye reaction mix using the vector primers and four internal primers oriented in both directions. Sequences derived from metazoan hosts were detected by BLAST analysis. Four new gregarine sequences were deposited in GenBank (Accession numbers DQ093793-DQ093796).

The four new sequences were aligned with 52 other alveolate sequences using MacClade 4 (Maddison and Maddison 2000) and visual fine-tuning. Maximum likelihood (ML) and distance methods under different DNA substitution models were performed on the 56-taxon alignment containing 1163 unambiguous sites. Although all gaps were excluded from the alignment prior to phylogenetic analysis, signature indels for some clades could be easily discerned from viewing the alignment (available upon request). The alpha shape parameters were estimated from the data using HKY and a gamma distribution with invariable sites and eight rate categories (alpha = 0.37; Ti/Tv = 1.83; fraction of invariable sites = 0). Gamma-corrected ML trees (analyzed using the parameters listed above) were constructed with PAUP* 4.0 using the general time reversible (GTR) model for base substitutions (Posada and Crandall 1998; Swofford 1999). Gamma corrected ML tree topologies found with HKY and GTR were identical. ML bootstrap analyses were performed in PAUP* 4.0 (Swofford 1999) on one hundred re-sampled datasets under an HKY model using the alpha shape parameter and transition/transversion ratio (Ti/Tv) estimated from the original dataset.

Distances for the SSU rDNA dataset were calculated with TREE-PUZZLE 5.0 using the HKY substitution matrix (Strimmer and Von Haeseler 1996) and with PAUP* 4.0 using the GTR model. Distance trees were constructed with weighted neighbor joining (WNJ) using Weighbor (Bruno et al. 2000). Five hundred bootstrap datasets were generated with SEQBOOT (Felsenstein 1993). Respective distances were calculated with the shell script 'puzzleboot' (M. Holder and A. Roger, www.tree-puzzle.de) using the alpha shape parameter and transition/transversion ratios estimated from the original dataset and analyzed with Weighbor.

We also examined the 56-taxon dataset with Bayesian analysis using the program MrBayes 3.0 (Huelsenbeck and Ronquist 2001). The program was set to operate with GTR, a gamma distribution and four MCMC chains (default temperature = 0.2). A total of 11,000,000 generations were calculated with trees sampled every 100 generations and with a prior burn-in of 20,000 generations. The approximate $-\ln L$ value converged at a value of 15,315. Sampled trees were imported into PAUP*, and a majority rule consensus tree was constructed from 200 post-burn-in trees. Posterior probabilities were derived from the number of trees that displayed the most commonly encountered branching pattern for the particular nodes in question.

Concordant tree topologies produced by different methods are evident from the bootstrap statistics and posterior probabilities shown in Figure 3. Bootstrap values and posterior probabilities are absent from nodes that were not concordant in all analyses. Weakly supported molecular phylogenetic relationships, when they existed, are evident in Figures 3 and 4. We chose to emphasize these weak relationships instead of trying to provide tenuous resolution using tree topology tests (e.g. AU tests). In our view, the integration of different sources of data (e.g. ultrastructural and behavioral information) are more compelling grounds for assessing weakly supported nodes in molecular phylogenies.

GenBank accession numbers: (AF494059) *Adelina bambarooniae*, (AF274250) *Amphidinium asymmetricum*, (AY603402) *Babesia bigemina*, (M97909) *Blepharisma americanum*, (M97908) *Colpoda inflata*, (AY234843) *Colpodella edax*, (AY078092) *Colpodella pontica*, (AF330214) *Colpodella tetrahymenae*, (L19068) *Cryptosporidium baileyi*, (M64245) *Crypthecodinium cohnii*, (AF093489) *Cryptosporidium parvum*, (AF093502) *Cryptosporidium serpentis*, (AF39993) *Cytauxzoon felis*, (U67121) *Eimeria tenella*, (AF372772, AF372779, AF372780, AF372785, AF372786, AY179975, AY179976, AY179977, AY179988) Environmental sequences, (AF022155) *Gonyaulax spinifera*, (AF129882) *Gregarina niphandrodes*, (AJ415513) *Gymnodinium sanguineum*, (AF274261) *Gyrodinium dorsum*, (AF286023) *Hematodinium* sp., (AF130361) *Hepatozoon catesbianae*, (AF274268) *Kryptoperidinium foliaceum*, (DQ093796) *Lankesteria abbotti*, (AY116614) *Lankesteria* sp. from *Clavelina picta*, (AF080611) *Lankesterella minima*, (AY196706) *Lecudina polymorpha* morphotype 1, (AF457128) *Lecudina tuzetae*, (AF457130) *Leidyana migrator*, (AF521100) *Lessardia elongata*, (DQ093795) *Lithocystis* sp., (AB000912) Marine parasite from *Tridacna crocea*, (AY334568) *Mattesia geminata*, (AF457127) *Monocystis agilis*, (AJ271354) *Neospora caninum*, (AF022200) *Noctiluca scintillans*, (AF129883) *Ophryocystis elektroscirrha*, (M14601) *Oxytricha nova*, (X03772) *Paramecium tetraurelia*, (AF126013) *Perkinsus marinus*, (AY033488) *Pfiesteria piscicida*, (Y16233) *Prorocentrum panamensis*, (DQ093794) *Pterospora floridiensis*, (DQ093793) *Pterospora schizosoma*, (M64244) *Sarcocystis muris*, (AF274276) *Scrippsiella sweeneyae*, (AY196709) *Selenidium terebellae*, (AF013418) *Theileria parva*, (M97703) *Toxoplasma gondii*.

Acknowledgements

We wish to thank the staff at the Bamfield Marine Sciences Centre (British Columbia, Canada) and M. Berbee (Department of Botany, University of British Columbia, Canada) for providing the resources necessary for the collection of *Brisaster latifrons*. We also thank H. Esson for her assistance in collecting marine invertebrates near Bamfield. This work was supported by a grant to B. S. Leander from the National Science and Engineering Research Council of Canada (NSERC 283091-04) and by an NSERC Undergraduate Student Research Award to S. Lloyd. B. S. Leander is a Scholar of the Canadian Institute for Advanced Research.

References

Berney C, Fahrni J, Pawlowski J (2004) How many novel eukaryotic 'kingdoms'? Pitfalls and limitations of environmental DNA surveys. BMC Biol **2**: 13

Bower SM, Carnegie RB, Goh B, Jones SRM, Lowe GJ, Mak MWS (2004) Preferential PCR ampification of protistan small subunit rDNA from metazoan tissues. J Eukaryot Microbiol **51**: 325—332

Brownell C, McCauley JE (1971) Two New Gregarine Parasites from the Spatangoid-urchin *Brisaster latifrons*. Oregon State University, Corvallis, Department of Oceanography, pp 1—14

Brugerolle G (2002a) *Colpodella vorax*: ultrastructure, predation, life-cycle, mitosis and phylogenetic relationships. Europ J Protistol **38**: 113—126

Brugerolle G (2002b) *Cryptophagus subtilis*: a new parasite of cryptophytes affiliated with the Perkinsozoa lineage. Europ J Protistol **37**: 379—390

Brugerolle G, Mignot JP (1979) Observations sur le cycle l'ultrastructure et la position systématique de *Spiromonas perforans* (Bodo perforans Hoolande 1938), flagellé parasite de *Chilomonas parameciu*m: ses relations avec les dinoflagellés et sporozoaires. Protistologica **15**: 183—196

Bruno WJ, Socci ND, Halpern AL (2000) Weighted neighbor joining: a likelihood-based approach to distance-based phylogeny reconstruction. Mol Biol Evol **17**: 189—197

Carreno RA, Martin DS, Barta JR (1999) *Cryptosporidium* is more closely related to the gregarines than to coccidia as shown by phylogenetic analysis of apicomplexan parasites inferred using small-subunit ribosomal RNA gene sequences. Parasitol Res **85**: 899—904

Cavalier-Smith T (2004) Only six kingdoms of life. Proc R Soc Lond B **271**: 1251—1262

Cavalier-Smith T, Chao EE (2004) Protalveolate phylogeny and systematics and the origins of Sporozoa and dinoflagellates (phylum Myzozoa nom. nov.). Europ J Protistol **40**: 185—212

Coulon P, Jangoux M (1987) Gregarine species (Apicomplexa) parasitic in the burrowing echinoid *Echinocardium cordatum*: occurrence and host reaction. Dis Aquat Org **2**: 135—145

Cox FEG (1994) The evolutionary expansion of the sporozoa. Int J Parasitol **24**: 1301—1316

Dawson SC, Pace NR (2002) Novel kingdom-level eukaryotic diversity in anoxic environments. Proc Natl Acad Sci USA **99**: 8324—8329

Diez B, Pedros-Alio C, Massana R (2001) Study of genetic diversity of eukaryotic picoplankton in different oceanic regions by small-subunit rRNA gene cloning and sequencing. Appl Environ Microbiol **67**: 2932—2941

Dyson J, Grahame J, Evennett PJ (1993) The mucron of the gregarine *Digyalum oweni* (Protozoa, Apicomplexa), parasitic in *Littorina* species (Mollusca, Gastropoda). J Nat Hist **27**: 557—564

Dyson J, Grahame J, Evennett PJ (1994) The apical complex of the gregarine *Digyalum oweni* (Protozoa, Apicomplexa). J Nat Hist **28**: 1—7

Edgcomb VP, Kysela DT, Teske A, de Vera Gomez A, Sogin ML (2002) Benthic eukaryotic diversity in the Guaymas Basin hydrothermal vent environment. Proc Natl Acad Sci USA **99**: 7658—7662

Felsenstein J (1993) PHYLIP (Phylogeny Inference Package). University of Washington, Seattle

Grassé P-P (1953) Classe des grégarinomorphes (Gregarinomorpha n. nov.; Gregarinae Haeckel, 1866; gregarinidea Lankester, 1885; grégarines des auteurs). In: Grassé P-P (ed) Traité de Zoologie, vol 1. Masson, Paris, pp 590—690

Heintzelman MB (2004) Actin and Myosin in *Gregarina polymorpha*. Cell Motil Cytoskel **58**: 83—95

Heller G, Weise RW (1973) A scanning electron microscope study on *Gregarina* sp from *Udeopsylla nigra*. J Protozool **20**: 61—64

Huelsenbeck JP, Ronquist F (2001) MrBayes: Bayesian inference of phylogenetic trees. Bioinformatics **17**: 54—755

Kuvardina ON, Leander BS, Aleshin VV, Mylnikov AP, Keeling PJ, Simdyanov TG (2002) The phylogeny of colpodellids (Eukaryota, Alveolata) using small subunit rRNA genes suggests they are the free-living ancestors of apicomplexans. J Eukaryot Microbiol **49**: 498—504

Landers SC (1991) *Pterospora demodendrion* sp. nov. and *Pterospora clymenellae*, acephaline eugregarines from coastal North Carolina. Europ J Protistol **27**: 55—59

Landers SC (2001) *Pterospora floridiensis*, a new species of acephaline gregarine (Apicomplexa) from the maldanid polychaete *Axiothella mucosa* in St. Andrew Bay, Florida. Syst Parasitol **48**: 55—59

Landers SC, Gunderson J (1986) *Pterospora schizosoma*, a new species of aseptate gregarine from the coelom of *Axiothella rubrocincta* (Polychaeta, Maldanidae). J Protozool **33**: 297—300

Landers SC, Leander BS (2005) Comparative surface morphology of marine coelomic gregarines (Apicomplexa, Urosporidae): *Pterospora floridiensis* and *Pterospora schizosoma*. J Eukaryot Microbiol **52**: 23—30

Leander BS, Keeling PJ (2003) Morphostasis in alveolate evolution. Trends Ecol Evol **18**: 395—402

Leander BS, Keeling PJ (2004) Early evolutionary history of dinoflagellates and apicomplexans (Alveolata) as inferred from hsp90 and actin phylogenies. J Phycol **40**: 341—350

Leander BS, Clopton RE, Keeling PF (2003a) Phylogeny of gregarines (Apicomplexa) as inferred from SSU rDNA and beta-tubulin. Int J Syst Evol Microbiol **53**: 345—354

Leander BS, Harper JT, Keeling PJ (2003b) Molecular phylogeny and surface morphology of marine aseptate gregarines (Apicomplexa): *Lecudina* and *Selenidium*. J Parasitol **89**: 1191—1205

Leander BS, Kuvardina ON, Aleshin VV, Mylnikov AP, Keeling PJ (2003c) Molecular phylogeny and surface morphology of *Colpodella edax* (Alveolata): insights into the phagotrophic ancestry of apicomplexans. J Eukaryot Microbiol **50**: 334—340

Levine ND (1971) Taxonomy of the Archigregarinorida and Selenidiidae (Protozoa, Apicomplexa). J Protozool **18**: 704—717

Levine ND (1976) Revision and checklist of the species of the aseptate gregarine genus *Lecudina*. Trans Am Microsc Soc **95**: 695—702

Levine ND (1977a) Checklist of the species of the aseptate gregarine family Urosporidae. Int J Parasitol **7**: 101—108

Levine ND (1977b) Revision and checklist of the species (other than *Lecudina*) of the aseptate gregarine family Lecudinidae. J Protozool **24**: 41—52

Levine ND (1981) New species of *Lankesteria* (Apicomplexa, Eugregarinida) from ascidians on the central California coast. J Protozool **28**: 363—370

Lopez-Garcia P, Rodriguez-Valera F, Pedros-Alio C, Moreira D (2001) Unexpected diversity of small eukaryotes in deep-sea antarctic plankton. Nature **409**: 603—607

MacGregor HC, Thomas PA (1965) The fine structure of two archigregarines, *Selenidium fallax* and *Ditrypanocystis cirratuli*. J Protozool **12**: 438—443

MacMillan WG (1973) Conformational changes in the cortical region during peristaltic movements of a gregarine trophozoite. J Protozool **20**: 267—274

Maddison DR, Maddison WP (2000) MacClade 4.05 OSX. Sinauer Associates, Inc., Sunderland, MA

Mellor JS, Stebbings H (1980) Microtubules and the propagation of bending waves by the archigregarine, *Selenidium fallax*. J Exp Biol **87**: 149—161

Moreira D, López-García P (2002) The molecular ecology of microbial eukaryotes unveils a hidden world. Trends Microbiol **10**: 31—38

Moreira D, Lopez-Garcia P (2003) Are hydrothermal vents oases for parasitic protists? Trends Parasitol **19**: 556—558

Morrissette NS, Sibley LD (2002) Cytoskeleton of apicomplexan parasites. Microbiol Mol Biol Rev **66**: 21—38

Mylnikov AP (1991) The ultrastructure and biology of some representatives of order Spiromonadida (Protozoa). Zool Zhur **70**: 5—15

Mylnikov AP (2000) The new marine carnivorous flagellate *Colpodella pontica* (Colpodellida, Protozoa). Zool Zhur **79**: 261—266

Mylnikov AP, Mylnikova ZM, Tsvetkov IA (1998) The fine structure of carnivorous flagellate *Colpodella edax*. Biologiya Vnutrenich Vod Sankt-Petersburg **3**: 55—62

Perkins FO (1976) Zoospores of the oyster pathogen, *Dermocystidium marinum*. I. Fine structure of the conoid and other sporozoan-like organelles. J Parasitol **62**: 959—974

Perkins FO (1996) The structure of *Perkinsus marinus* (Mackin, Owen and Collier, 1950) Levine, 1978 with comments on the taxonomy and phylogeny of *Perkinsus* spp J Shell Res **15**: 67—87

Posada D, Crandall KA (1998) MODEL TEST: testing the model of DNA substitution. Bioinformatics **14**: 817—818

Ray HN (1930) Studies on some protozoa in polychaete worms. I. Gregarines of the genus *Selenidium*. Parasitology **22**: 370—400

Schrével J (1968) L'ultrastructure de la région antérieure de la grégarine *Selenidium* et son intérêt pour l'étude de la nutrition chez les sporozoaires. J Microscopie **7**: 391—410

Schrével J (1970) Contribution a l'étude des Selenidiidae parasites d'annélides polychètes. I. Cycles biologiques. Protistologica **6**: 389—426

Schrével J (1971a) Contribution a l'étude des Selenidiidae parasites d'annélides polychètes. II. Ultrastructure de quelques trophozoïtes. Protistologica **7**: 101—130

Schrével J (1971b) Observations biologique et ultrastructurales sur les Selenidiidae et leurs conséquences sur la systématique des grégarinomorphes. J Protozool **18**: 448—470

Siddall ME, Reece KS, Nerad TA, Burreson EM (2001) Molecular determination of the phylogenetic position of a species in the genus *Colpodella*. Am Mus Novitat **3314**: 1—10

Simpson AGB, Patterson DJ (1996) Ultrastructure and identification of the predatory flagellate *Colpodella pugnax* Cienkowski (Apicomplexa) with a description of *Colpodella turpis* n. sp. and a review of the genus. Syst Parasitol **33**: 187—198

Stach T, Turbeville JM (2002) Phylogeny of Tunicata inferred from molecular and morphological characters. Mol Phylogenet Evol **25**: 408—428

Stebbings H, Boe GS, Garlick PR (1974) Microtubules and movement in the archigregarine, *Selenidium fallax*. Cell Tiss Res **148**: 331—345

Strimmer K, Von Haeseler A (1996) Quartet Puzzling: a quartet maximum likelihood method for reconstructing tree topologies. Mol Biol Evol **13**: 964—969

Swofford DL (1999) Phylogenetic Analysis using Parsimony (and other methods) PAUP* 40. Sinauer Associates, Inc., Sunderland, MA

Vavra J, Small EB (1969) Scanning electron microscopy of gregarines (Protozoa, Sporozoa) and its contribution to the theory of gregarine movement. J Protozool **16**: 745—757

Vivier E (1968) L'organization ultrastructurale corticale de la gregarine *Lecudina pellucida*: ses repports avec l'alimentation et la locomotion. J Protozool **15**: 230—246

Vivier E, Schrével J (1964) Étude, au microscope électronique, d'une grégarine du genre *Selenidium*, parasite de *Sabellaria alveolata* L. J Microscopie **3**: 651—670

Vivier E, Schrével J (1966) Les ultrastructures cytoplasmiques de *Selenidium hollandei*, n. sp. grégarine parasite de *Sabellaria alveolata* L. J Microscopie **5**: 213—228

Warner FD (1968) The fine structure of *Rhynchocystis pilosa* (Sporozoa, Eugregarinida). J Protozool **15**: 59—73

Wray CG, Langer MR, DeSalle R, Lee JJ, Lipps JH (1995) Origin of the foraminifera. Proc Natl Acad Sci USA **92**: 141—145